

A Level Set Study of Shear-driven Contact Line Dynamics

Kurt Smith

A summary of work performed at Unilever Research, Port Sunlight, UK

Advisors: Patrick Warren, Janette Jones

July 12 – August 17, 2002

Synopsis

The aim of this internship was to apply numerical methods developed during my thesis research to a problem of interest to the modeling group at Unilever. Unilever is a multinational company which develops and markets foods and home & personal care products (soaps, lotions, detergent, etc.). Basic scientific research is performed at Port Sunlight and other locations. The group I worked with does numerical modeling of various problems ranging from molecular to macroscopic scales. My time spent at Unilever had the dual benefits of bringing new ideas into the modeling group and broadening the scope of my thesis research. In conversations with Dr. Warren prior to my arrival we settled on the problem of the moving contact line as a relevant topic of study. This is a classical physical problem which is of interest to Unilever in the spreading of liquid soaps and lotions on various surfaces.

Previously this topic had been studied in the group with mesoscopic numerical methods (namely dissipative particle dynamics and lattice-Boltzmann techniques) in which a collection of mesoscopic, or coarse-grained, particles interact according to some set of rules. These methods are valuable because they capture some degree of the small scale details of a system without being as intensive as molecular dynamics. In many situations (for instance in the formation of lamellar phases of diblock copolymers or other dimers) this approach is more practical than the typical macroscopic approach of solving a set of differential equations with finite-difference or finite-element methods. One of the drawbacks of mesoscopic methods in fluid systems is that it is often difficult to extract a velocity field or fluid interface with decent resolution, due to fluctuations. This has made it difficult to measure a contact angle or describe the flow field near the contact line. In my thesis work I have developed a Navier-Stokes solver which uses a level set algorithm to track the interface between immiscible fluids. I have used this method to study fluid interfaces (such as droplets) in shear flows. It is well suited to determining the precise interface shape and the corresponding flow field.

My work at Unilever had two components. I first conceived a phenomenological rule for contact line motion and implemented it in the level set code. After this was accomplished I collected results for a simple system in order to describe the flow near a contact line and also to verify an analytical argument proposed for the balance of forces in the system. This work is described below. In addition to work on the contact line problem there were many other benefits to my time at Unilever. I spoke to a wide range of scientists, many of whom were interested in applying the level set code in new areas (such as thin films and membranes). I also gained a better idea of the type of work that is possible in an industrial research setting. Finally I was able to make contacts in Europe (not only at Unilever but also at several academic centers) which will be valuable when I begin a post-doctoral position in France next year.

Introduction

It has been known for some time [1] that the motion of a contact line leads to a force singularity in the Navier-Stokes equations if a no-slip boundary condition at the solid surface is assumed. This fact has led to the proposal of various microscopic mechanisms (such as molecular diffusion or evaporation-condensation) by which contact line motion could occur [2].

Recently several numerical techniques have been used to simulate a dynamic contact line. These range from molecular dynamics [3] to mesoscopic models (such as lattice Boltzmann [4], diffuse interface [5], and dissipative particle dynamics [6]) to macroscopic sharp interface methods [7]. Each of these methods carries advantages and disadvantages. Molecular scale simulations capture the most physical detail and thus can be expected to most accurately reproduce the dynamics where a macroscopic governing equation is unknown. However their computational intensity prohibits simulations of large length and time scales which are often of practical interest. Mesoscopic models provide a useful tradeoff by reducing the amount of detail while still giving rise to behavior such as contact line motion implicitly. Macroscopic techniques face the most difficulty because they contain no mechanism for producing contact line motion. Instead some type of slip velocity must be explicitly specified. However these methods are widely used to study practical systems containing immiscible fluids. They have the advantage of providing an unambiguous description of the velocity field and interface location. Thus in many applications it would be valuable to be able to treat contact line motion accurately within a macroscopic model.

In this paper we consider one such macroscopic model, a finite difference Navier-Stokes solver paired with a level set method to track the evolution of the free surface (NSLSM). This method has been shown to handle free surface flows accurately [8] including instances of breakup and coalescence. Recently the level set method has been extended to handle multiple junctions formed by three or more immiscible fluids [9]. We have modified the NSLSM to handle contact lines with slip velocity as described below. This technique has been applied to a contact line scenario for which we provide a theoretical argument for the force balance in the vicinity of the contact line.

System description

We consider two immiscible fluids occupying a two dimensional region between parallel plates located at $y=0,L$ such that the interface separating the two fluids forms a contact line at either plate (Figure 1a). Periodic boundaries in the x direction are implemented. The plates are moved in opposite directions at constant velocities. Assuming inertial effects are small ($Re \rightarrow 0$) there are three forces acting on the system- viscous shear stresses, surface tension, and a slip force located at the contact line. For small velocities a linear relation between the slip velocity U_{slip} and contact angle θ is a reasonable assumption [10]:

$$(1) U_{slip} = k(\theta_{eq}-\theta)/\theta_{eq}$$

where θ_{eq} is the equilibrium contact angle given by the Young-Laplace condition. Our code follows the lines of [8] and [9] in which an interface, Γ , is defined as the zero contour of a function $\phi(\mathbf{x},t)$. In the interior of the fluid ϕ is advected with the continuum fluid velocity \mathbf{u} . The slip velocity is considered to be separate from \mathbf{u} . Thus the velocity of the interface at the wall is $(U_{wall}+U_{slip},0)$ while the boundary condition for the fluid velocity is $\mathbf{u}=(U_{wall},0)$. The angle θ is determined by measuring the slope from the location of the interface at the wall and one cell length away from the wall.

The balance of forces in the system is characterized by two dimensionless parameters: a capillary number $Ca=\eta U_{wall}/\sigma$, and a dimensionless slip velocity $\beta=k/U_{wall}$. η is the fluid viscosity and σ is surface tension. One additional parameter, $p=X/L$ (where X is the distance in the x direction between adjacent interfaces), completes the description of the system. We consider a symmetrical system where $\theta_{eq}=\pi/2$ and viscosity in both phases is equal. Then the four contact lines in Figure 1a are equivalent and, additionally, have a similarity to the rear contact line of a drop moving down an inclined surface (Figure 1(b)).

In order for a steady state to be reached both Ca and β^{-1} must be sufficiently small, that is, both slip and surface tension forces play a role in opposing shear. In the limit that $Ca \rightarrow \infty$ the contact line undergoes continuous motion. Since surface tension is negligible an angle of θ_{eq} can be maintained by large interfacial curvature near the wall. In the limit that $\beta^{-1} \rightarrow \infty$ the the contact line always moves with the wall velocity since slip is not possible.

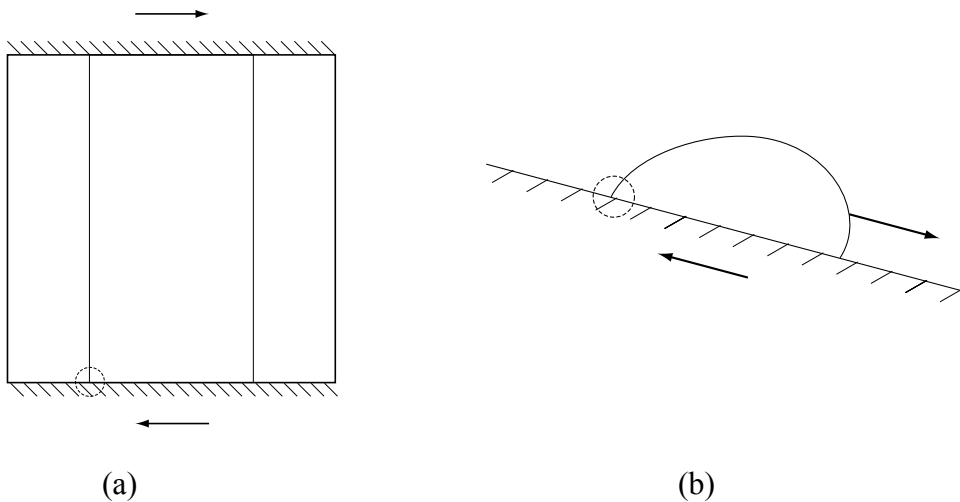


Figure 1. (a) Shear driven interface. Local dynamics at the contact line are similar to those at the rear contact line of a droplet moving down an inclined surface (b).

Results and Discussion

1. Steady and Unsteady Flow fields

Typical steady state flow fields for $p=1/2$ and $p=1$ are shown in Figures 2 and 3 respectively. It is interesting to note that the flow in a given phase (i.e. between two adjacent interfaces) resembles a driven cavity flow. At steady state the fluid interfaces play a role similar to the side walls in a driven cavity, the main difference being that the tangential component of velocity can be non-zero on the interface. For $p=1/2$ there are two main cells in a fluid phase, one at top and one at bottom. For $p=1$ the two cells merge (except near the center of the phase) so that over most of the fluid there is a single circulating flow. This is similar to the change in driven cavity flow when the aspect ratio is varied. In Figure 2 the midpoint of an interface, M , is a hyperbolic point whose stable manifolds originate at the contact lines and whose unstable manifolds are directed towards the center of each phase. This produces the secondary cells seen in Figure 2(b) which would not exist in a driven cavity. For $p=1$ the unstable manifolds of M are directed towards the contact lines. In this case the secondary cells are much narrower and are difficult to visualize at this resolution.

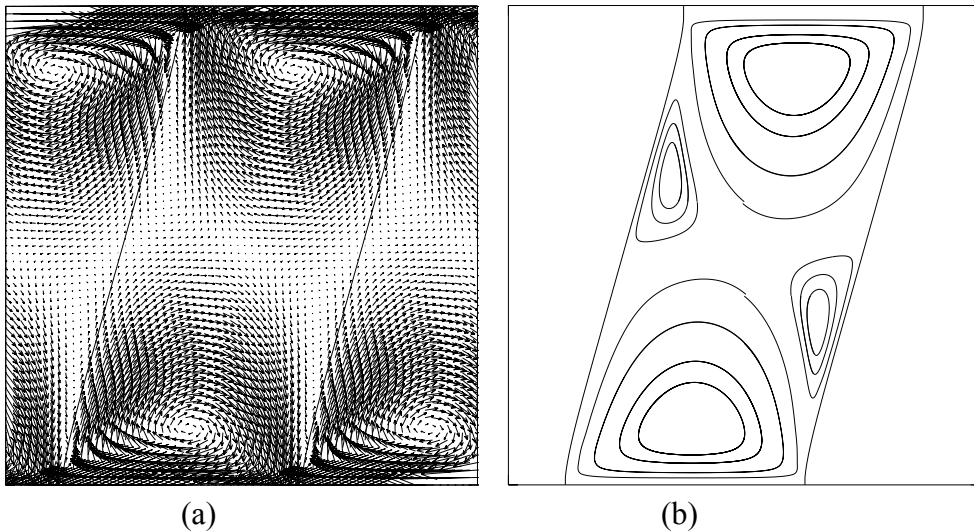
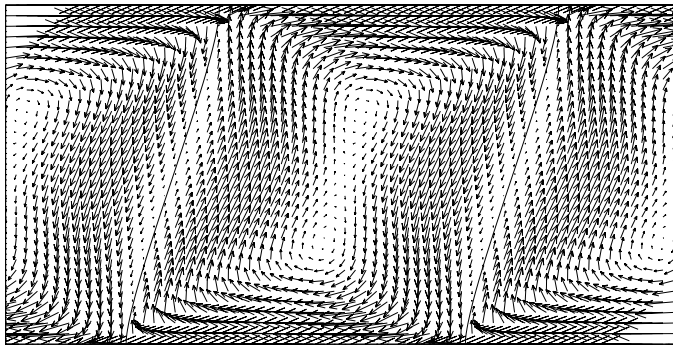
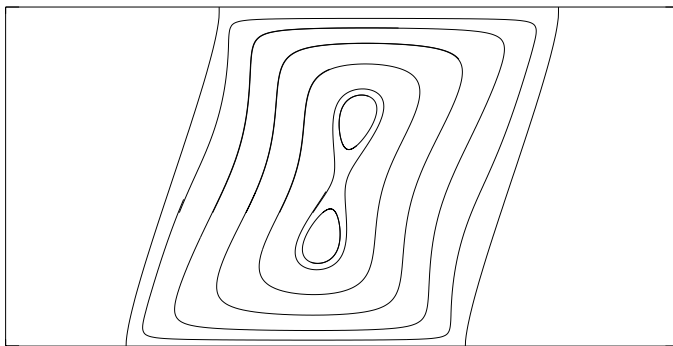


Figure 2. Steady flow for a periodic system with $p=1/2$. $Ca=0.05$, $\beta=400$. (a) velocity field ; (b) streamlines. Flow at the top wall is to the left and at the bottom wall to the right.



(a)



(b)

Figure 3. Steady flow for a periodic system with $p=1$. $Ca=0.05$, $\beta=20$. (a) velocity field ; (b) streamlines. Flow at the top wall is to the left and at the bottom wall to the right.

In Figure 4 a close-up of the flow field near a contact line from Figure 2 is shown. The fluid on the right undergoes a “caterpillar” motion as described by Dussan [11] in which fluid elements lying on the wall approach the contact line where they are then lifted off the wall and move along the fluid/fluid interface. A necessary condition for this flow is the existence of an injected streamline in the left hand fluid which flows towards the contact line, as is clearly seen in the figure. The resulting flow is similar to Figure 8 in [11].

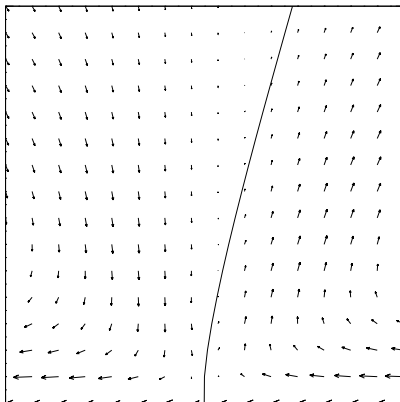


Figure 4. Steady flow field in the vicinity of a contact line. $Ca=0.05$

Previous work has mainly described the steady flow in the reference frame of the contact line, where the interface maintains a constant dynamic contact angle (θ_d). In our simulations we are also able to observe the evolution of the flow towards this steady state. An example is shown in Figure 5. As the interface moves the flow near the wall develops a “hump” which grows along the interface. Flow across the interface is largest at the tip of the hump. At some point the tip splits (in our system this occurs when the humps from the upper and lower contact lines intersect) and the interface attains a steady shape.

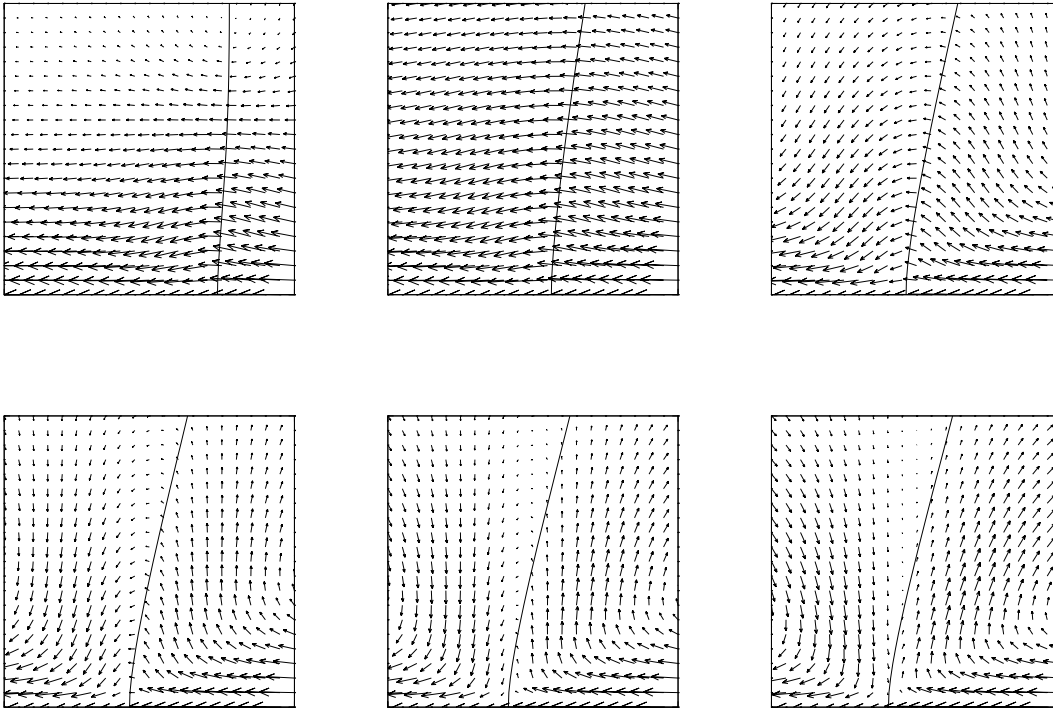


Figure 5. Evolution to steady state flow for a contact line subjected to sudden shear.

2. Force Balance

In this section we describe the balance of forces in the contact region and derive the relation of the apparent contact angle to Ca and β . For the contact line to be stationary in the system frame of reference it is necessary that $U_{\text{slip}} + U_{\text{wall}} = 0$. Thus from (1) it follows that the dynamic contact angle depends on β as:

$$(2) \theta_d/\theta_{\text{eq}} = 1 - \beta^{-1}$$

We first consider the limit $\beta \rightarrow \infty$ so that $\theta_d/\theta_{\text{eq}} = 1$. In an outer region, away from the contact line, the interface is nearly straight. The slope of the interface in this region defines an apparent contact angle θ_a which differs from θ_d . The value of θ_a depends on

surface tension forces in the contact region, where the interface has large curvature. We approximate the interface as a two straight segments so that it has an angle of θ_a outside of a region of length h from the wall as shown in Figure 6. Then curvature is concentrated over an infinitesimally small length. Surface tension can be treated as a point force located at a height h and from geometrical arguments it can be shown to have the form:

$$(3) \mathbf{F}_{\text{surf}} \propto \sigma(\cos \theta_a, \sin \theta_a - 1)$$

Since the point is stationary in the system frame of reference the horizontal component of \mathbf{F}_{surf} must be balanced by a hydrodynamic drag force:

$$(4) \sigma \cos \theta_a \propto \eta U_{\text{wall}}$$

or:

$$(5) \cos \theta_a \propto Ca$$

For finite values of β this picture is slightly changed as shown in Figure 6(b). In this case the horizontal component of \mathbf{F}_{surf} is

$$(6) \mathbf{F}_x = \sigma(\cos \theta_a - \cos \theta_d)$$

and the appropriate expression for θ_a becomes

$$(7) \cos \theta_a = \cos([1 - \beta^{-1}]\theta_{\text{eq}}) + K \cdot Ca$$

where K is a constant.

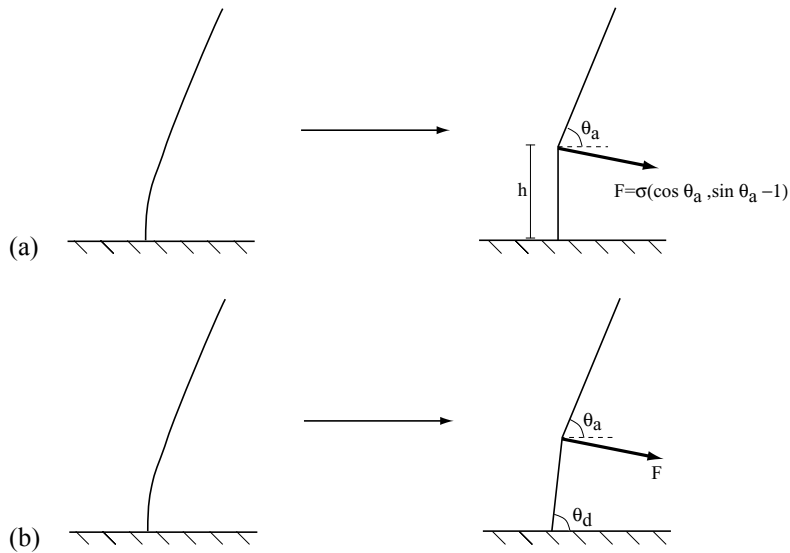


Figure 6. Approximation of curvature in contact region as a point force for $\beta \rightarrow \infty$ (a) and for finite β (b).

To verify these predictions numerically a series of interface shapes were computed for several values of β and Ca . Interfacial profiles, presented here as the variation of the interfacial angle θ along the length of the interface, are shown in Figures 7 and 8. In all cases the interface is nearly flat away from the walls, where $\theta = \theta_a$. For small β the shape of the curve depends on Ca . This is because $\theta_d (= \theta(y=0))$ is determined by β while $\theta_a (= \max(\theta(y)))$ decreases with Ca . Thus the curves in Figure 7 have different values at the walls. In the large β limit, $\theta_d \approx \theta_{eq}$ and thus all curves in Figure 8 approach zero at the walls. θ_a is plotted against Ca in Figure 9. At the largest values of β the data is well described by (5) while for lower β an offset from the origin, as predicted by (7), can be seen in Figure 10. For all values of β the data appears to be linear with a slope of $K \approx 5.3$.

The physical significance of the length h is also of interest. It can be roughly thought of as the length scale over which wall interactions are significant. Numerically it scales with the grid resolution because the value of θ used in (1) is determined from information within one cell length from the wall. As resolution is increased the length of the contact region, over which there is significant interfacial curvature, should decrease. Ultimately, molecular scale phenomena near the contact line are beyond the reach of our macroscopic model. However our results show that the model provides a means to incorporate these phenomena into a macroscopic description of the fluid.

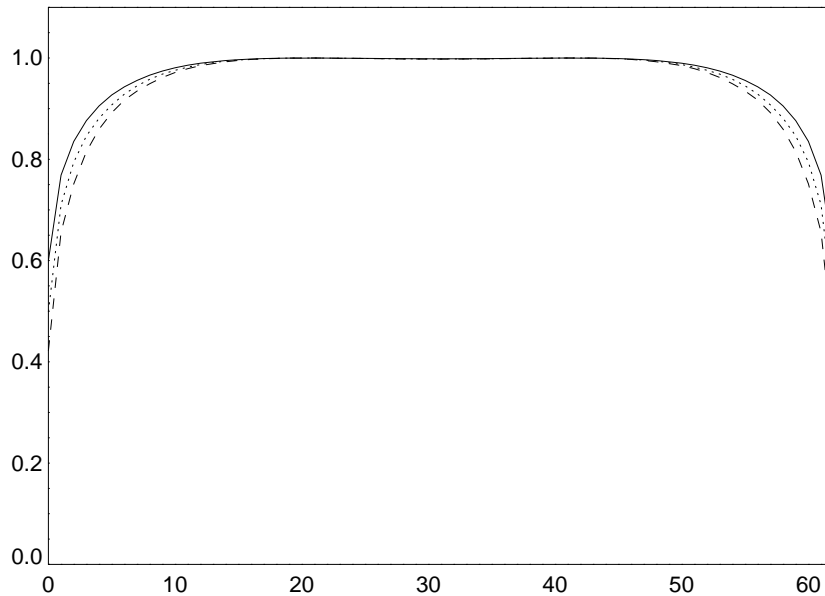


Figure 7. $[\theta_{eq} - \theta] / [\theta_{eq} - \theta_a]$ vs. y . $\beta = 20$. $Ca = 0.01$ (solid line); $Ca = 0.015$ (dotted line); $Ca = 0.02$ (dashed line).

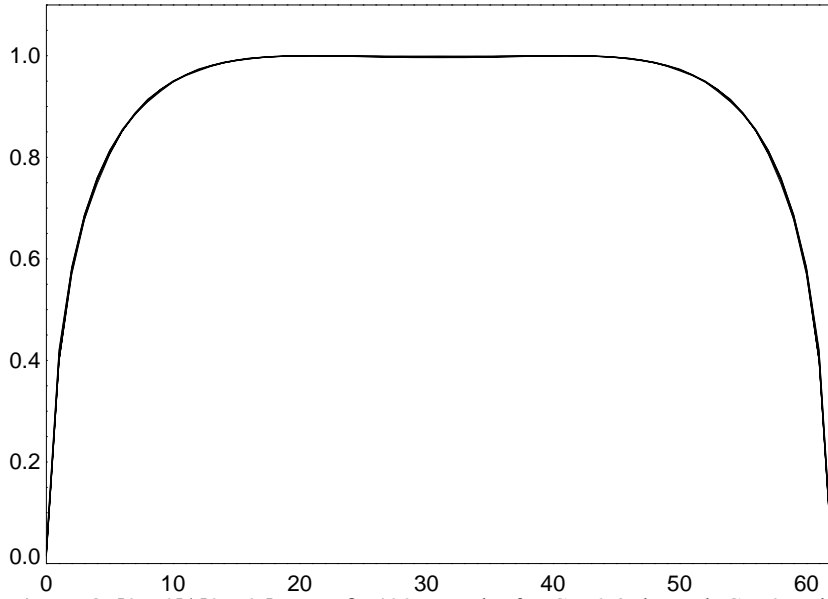


Figure 8. $[\theta_{eq}-\theta] / [\theta_{eq}-\theta_a]$ vs. y . $\beta=400$. Results for $Ca=0.2$ through $Ca=0.5$ shown. Data collapses onto a single curve.

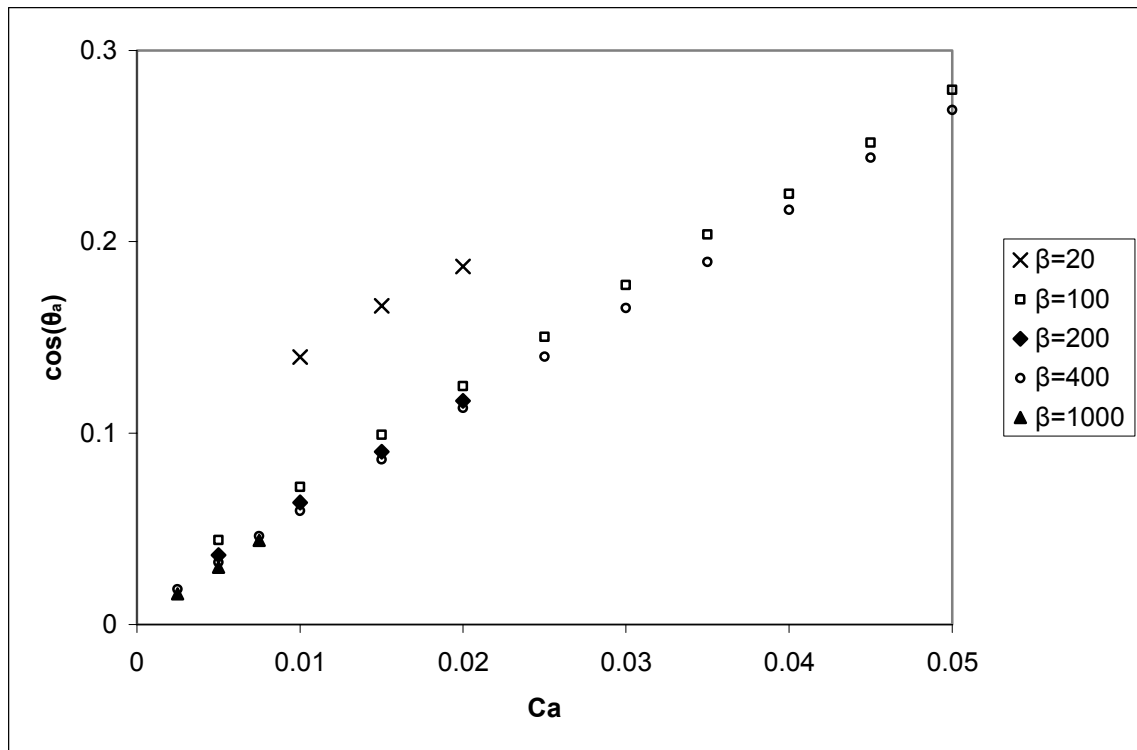


Figure 9. $\cos(\theta_a)$ vs. Ca for several values of β .

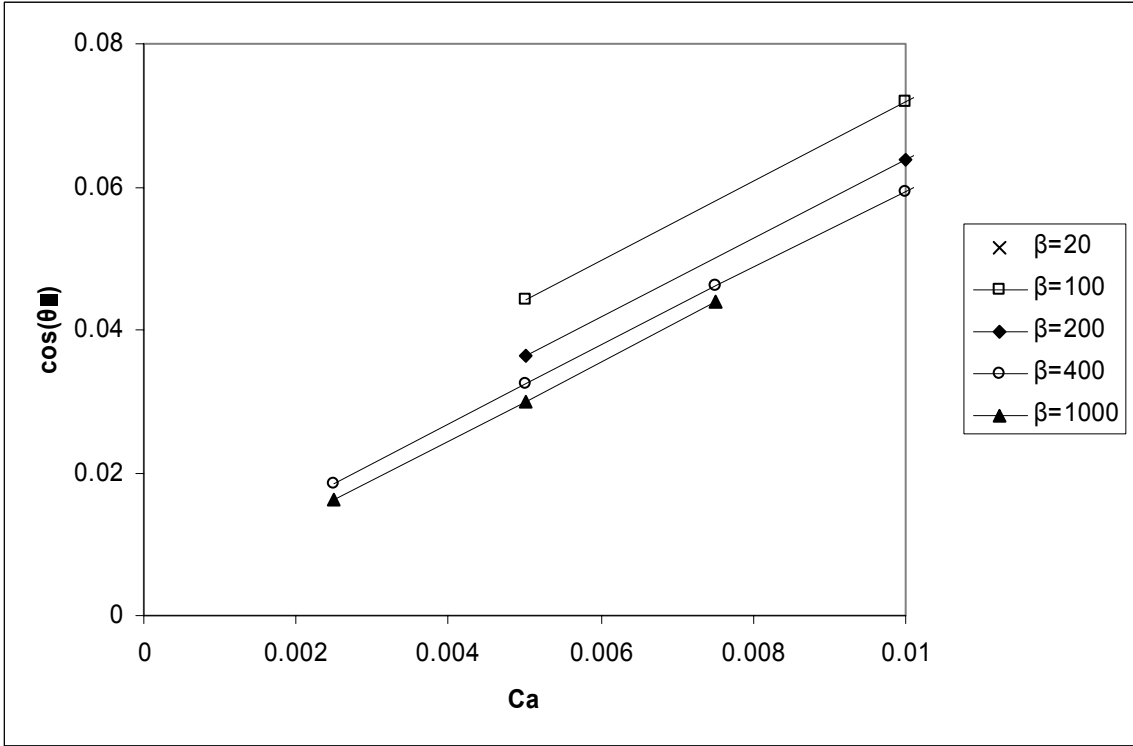


Figure 10. Close up of data from Figure 9.

References:

1. C. Huh and L.E. Scriven, "Hydrodynamic model of steady movement of a solid/liquid/fluid contact line", *J. Coll. Int. Sci.*, **35**, 85, 1971.
2. P. G. DeGennes , "Wetting- statics and dynamics" , *Rev. Mod. Phys.* , **57** , 827-863, 1985.
3. J. L. Barrat and L. Bocquet, "Large slip effect at a nonwetting fluid-solid interface", *Phys. Rev. Lett.*, **82**, 4671-4674, 1999.
4. A. J. Briant, P. Papatzacos and J. M. Yeomans, "Lattice Boltzmann simulations of contact line motion in a liquid-gas system", *Phil. Trans. Roy. Soc. A* , **360**, 485-495, 2002.
5. D. Jacqmin , "Contact-line dynamics of a diffuse fluid interface" , *J. Fluid Mech.*, **402**, 57-88 , 2000 ; H.Y. Chen, D. Jasnow and J. Vinals , "Interface and contact line motion in a two phase fluid under shear flow", *Phys. Rev. Lett.* , **85** ,1686-1689, 2000.
6. J. L. Jones, M. Lal, J. N. Ruddock and N. A. Spenley , "Dynamics of a drop at a liquid/solid interface in simple shear fields: A mesoscopic simulation study" ,*Farad. Disc.* , **112** , 129-142 , 1999.
7. M. Renardy, Y. Renardy and J. Li, "Numerical simulation of moving contact line problems using a volume-of-fluid method", *J. Comp. Sci.*, **171**, 243-263, 2001.
8. Y. C. Chang and T. Y. Hou and B. Merriman and S. Osher, "A level set formulation of eulerian interface capturing methods for incompressible fluid flows", *J. Comp. Phys.*, **124** , 449-464, 1996.
9. K. A. Smith, F. J. Solis and D. L. Chopp, "A projection method for motion of triple junctions by level sets", *Interf. Free Bound.*, **4**, 263-276, 2002.
10. Y Pomeau, "Recent progress in the moving contact line problem: a review", *C.R. Mecanique*, **330**, 207-222, 2002.
11. E. B. Dussan V., "On the spreading of liquids on solid surfaces: static and dynamic contact lines." *Ann. Rev. Fluid Mech.*, **11**, 371-400 1979.